Remote regulation of magnetic particle targeted Wnt signalling for bone tissue engineering

M Rotherham PhD[a*], JR Henstock PhD[a,1], O Qutachi PhD[b], AJ El Haj PhD[a]

[a]Institute for Science and Technology in Medicine, Keele University, Stoke-on-Trent, UK, ST4 7QB.

[b]School of Pharmacy, University of Nottingham, Nottingham, UK, NG7 2RD.

[1]Present address: Institute of Ageing and Chronic Disease, William Duncan Building, 6 West Derby Street, Liverpool, United Kingdom, L7 8TX

* Corresponding Author

Dr Michael Rotherham (Corresponding Author)

Institute for Science and Technology in Medicine - Keele University,

Guy Hilton Research Centre,

Thornburrow Drive, Hartshill

Stoke-on-Trent

ST4 7QB, UK

Tel: +44(0)1782 674988

Fax: +44 (0)1782 674467

E-mail: m.rotherham@keele.ac.uk

Word count (Abstract): 149

Word count (Manuscript): 4983

Number of figures: 6

Number of tables: 0

Number of references: 51

Number of Supplementary online-only files: 1

Related conference abstracts: TERMIS (EU) 2016 Conference (Poster presentation).

M Rotherham *et al*, (2016), European Cells and Materials Vol. 31. Suppl. 1, (page P388)

Funding bodies:

This research was funded by the BBSRC (grant number: BB/G010579/1) and the European Union's Horizon 2020 research and innovation programme (grant agreement n° 686841). The funding bodies had no involvement in the research and/or preparation of the article.

Conflicts of Interest: Alicia El Haj is a Director and co-founder of MICA Biosystems Ltd. She receives no salary and holds 50% of the shareholding in MICA Biosystems Ltd.

Abstract

Wnt signalling is critically involved in the differentiation of human Mesenchymal Stem Cells (hMSC). Wnt proteins therefore have considerable therapeutic value, but are expensive and difficult to produce. UM206 is a synthetic peptide and ligand for the Wnt receptor Frizzled. Attachment of UM206 to magnetic nanoparticles (MNP) enables the ligand-MNP complex to be manipulated using magnetic fields, allowing control of Frizzled stimulation. Using this approach, Wnt signalling was activated in hMSC which resulted in Frizzled clustering, β-catenin translocalisation and activation of TCF/LEF responsive transcription. During osteogenesis, UM206-MNP initiated localised mineralised matrix formation. Injection and magnetic stimulation of UM206-MNP-labelled MSC in *ex vivo* chick femurs resulted in increased mineralisation which acted synergistically with addition of bone morphogenic protein 2 (BMP2) releasing micro-particles. As this facilitates external control over signal transduction, conjugated MNP technology has applications both as a research tool and for regulating tissue formation in clinical cell therapies.

Key words: Mesenchymal stem cells; Magnetic nanoparticles; Wnt signalling; bone tissue engineering

Background

Human mesenchymal stem cells (hMSC) are a promising source for autologous cell therapies, particularly for orthopaedic tissue engineering [1]. MSC differentiation into osteoblasts results from an array of signalling cascades which are triggered by growth factors, physical and environmental stimuli which cross-talk with each other. These stimuli alter the expression of numerous regulatory factors including Wnt proteins. MSC have been shown to express a range of Wnt proteins and receptors and the pathway is a pivotal regulator of hMSC fate and osteoblast differentiation [2], [3].

Wnt signalling pathways have a multitude of effects on cell behaviour including changes to polarity and differentiation. The effects are dependent on cell type and Wnt protein context [4], [5]. For example activation of canonical signalling has been shown to promote hMSC proliferation, preserve multipotency and inhibit differentiation [6], [7]. However over-expression of the Wnt co-receptor LRP5 and active β-catenin has also been shown to promote osteogenic differentiation of hMSC [8]. Recently, we have demonstrated that immobilised Wnt molecules influence MSC migration and differentiation in 3D *in vitro* models [9]. *In vivo*, Wnt3A enhances skeletal progenitor cell proliferation, differentiation and accelerates bone repair in Axin2 knockout mice [10].

Despite the significant role of Wnt in directing tissue formation, its use *in vivo* for bone repair has been limited. This is partly due to the complex and costly production methods required to produce pharmacological quantities of bioactive Wnt with the appropriate post-translational modifications [11], [12]. Therefore, there is considerable interest in developing synthetic Wnt analogues to pharmacologically regulate Wnt signalling for therapeutic use. UM206 is a synthetic peptide based on a conserved fragment of Wnt3A and Wnt 5A. UM206 is a specific ligand for Frizzled1 and Frizzled2 receptors and is capable of activating canonical Wnt signalling depending on its conformation [13].

The use of magnetic nanoparticles (MNP) to target cell signalling pathways is an expanding research area in biomedical research. Our previous work has demonstrated the efficacy of remotely activating Wnt signalling using oscillating magnetic fields with antibody-coated MNP targeted against Frizzled2 receptors [14]. The use of magnetite MNP for biomedical applications is particularly attractive due to the level of control that can be excised over particle shape, size, charge, coating, magnetization and dose [15]. MNP have been used for biomedical applications such as control of cell function and positioning in conjunction with magnetic fields. This can enable formation of heterotypic co-culture cell layers and complex tissue formation [16], [17]. Incorporation of growth factor conjugated magnetite MNP into silk fibroin scaffolds has also shown efficacy in bone tissue engineering [18]. From a clinical perspective, the translational potential of magnetite based MNP is clear from their current use as MRI contrast agents [19]. A detailed review discussing the clinical applications of MNP in the context of orthopaedics is provided by Wimpenny *et al* [20]. We have demonstrated the potential applications of MNP in tissue engineering and regenerative medicine by targeting other mechanically responsive targets such as the TREK1 ion channel [21], [22], PDGF receptors [23] and Integrins [24].

In this study, we report on the feasibility of using synthetic peptide-MNP conjugates for remote signalling mechano-activation. Initially, we have demonstrated the mechanism of Frizzled signal transduction and Wnt pathway activation via UM206-conjugated MNP and oscillating magnetic fields in hMSC using reporter systems. The potential use of UM206-conjugated MNP for directing bone formation remotely was then assessed using *in vitro* monolayer and 3D (*ex vivo*) foetal chick femur models [25], [26]. The synergistic effects of MNP-mediated Wnt activation and BMP2 signalling on bone formation were also investigated. The overall aim of this research was to demonstrate that remote activation of Wnt signalling pathways in mesenchymal cell progenitors using peptide conjugated MNP can

regulate remote controlled bone tissue formation. This technique has applications in both *in vitro* basic research and in orthopaedic cell therapies.

Methods

Cell culture. hMSC were isolated from fresh bone marrow (Lonza) as described in supplementary methods. Cells were expanded in basal media (10% FBS, 1% L-glutamine and 1% penicillin/streptomycin) (Lonza). Media was replaced twice per week and cells P1-5 were used in all experiments. Osteogenic media was prepared as described in supplementary methods. For Wnt-treated control groups diluted Wnt3A conditioned media collected from Wnt3A overexpressing L-M (TK-) cells (LGC standards) was used.

Transient transfections. hMSC were transiently transfected with a Gaussia Luciferase reporter under control of a TCF/LEF promoter as described previously [14] and in supplementary methods.

MNP coating. 250nm SPIO carboxyl functionalised MNP (Micromod) were covalently coated with UM206 peptide by carbodiimide activation as described previously [14] (Fig. 1a) and in supplementary methods. MNP coating was characterised as described in the supplementary methods.

Cell labelling with MNP. Cells were cultured in reduced serum basal media for 3h prior to addition of 25μg MNP/2x10^5 cells. Cells were incubated with MNP for 1.5h, then washed with PBS to remove unbound particles before addition of fresh media (Fig. 1b).

Magnetic stimulation. Magnetically stimulated groups were treated with ≥25mT magnetic fields using an oscillating magnetic force bioreactor (MICA Biosystems) as described previously [14] (Fig 1c). Treatment was performed as described in supplementary methods.

Cell viability staining. Cells were labelled with MNP and treated with magnetic field stimulation as described above. After 14 days treatment, cells were washed with PBS then stained with a Live/dead assay as described in supplementary methods.

MTT assay. Cells were labelled with varying doses of L-/C-C-UM206-MNP or uncoated (blank) MNP (5μg to 300μg MNP/2x10^5 cells) or treated with varying doses of linear / cyclic UM206 peptide (1-100μg/mL). Magnetic field groups were treated with magnetic field stimulation as described above. After 14 days MTT assay was performed as described in supplementary methods.

Immunocytochemistry. MNP labelling of cells, β-catenin and Osteocalcin staining were assessed using immunofluorescence as described in supplementary methods.

Proximity ligation assay. Frizzled receptor clustering was assessed using a proximity ligation assay (PLA) (Duolink, Sigma). Cells were seeded onto glass coverslips (1cm^2) and labelled with MNP as described above; magnetically stimulated groups were treated for 3h. Cells were fixed with 90% methanol and blocked as above and MNP and Frizzled2 were visualised by staining as described in supplementary methods.

Luciferase reporter assays. Experiments were performed in reduced serum basal media. At each time point, media samples were taken and analysed for luciferase activity using a luciferase flash assay kit (Thermo Pierce) on a Biotek Synergy 2 plate reader. Luciferase activity was normalised to the total protein content of cell lysates.

Chick femur culture and microinjection. Foetal chick femurs were extracted and treated as previously described [22] and in supplementary methods.

BMP2 microparticle encapsulation. BMP2 microparticles were prepared as previously described [22] and in supplementary methods.

X-ray microtomography. Chick femurs were analysed using X-ray microtomography (μCT) as previously described [22] and in supplementary methods.

Histology. For *in vitro* experiments cells were fixed as above, washed with d.H_2O, then stained as described in supplementary materials. For chick femur experiments femurs were fixed in 4% paraformaldehyde for 48h, stored in PBS, then stained and sectioned as described in supplementary methods.

Immunohistochemistry. Femurs were processed as described in supplementary methods.

Statistical analysis. All data is presented as means +/- SEM. Statistical significance at 95% Confidence level was determined using 1-way ANOVA with post-hoc Tukey tests using Mini-tab. μCT data was analysed by 1-way ANOVA with post-hoc Dunnett's test, all groups were compared to the Sham injection (control) group.

Results

The MNP coating efficiency was first determined using total protein assay and physical characterisation. The amount of UM206 conjugated to MNP was estimated by measuring the protein content of the MNP coating solutions before and after incubation with activated MNP. The protein content of the coating solutions (ie. unbound protein) decreased by between 5% and 27% after incubation with the activated MNP (supplementary table 1). The hydrodynamic size and charge of L- / C-C-UM206 functionalised MNP were compared to uncoated-MNP. The hydrodynamic size of L- / C-C-UM206-MNP increased to between 332-345nm respectively, whilst surface charge increased to between -16 to -8mV. In contrast uncoated MNP had a hydrodynamic size of 299nm and a surface charge of -20mV (supplementary table 2).

RT-PCR was then used to confirm Frizzled2 expression in hMSC. Frizzled2 was found to be stably expressed over 21 days in basal or osteogenic media (Supplementary Fig. 1a). Furthermore Frizzled2 expression was found to be unaffected 24h after treatment with L- / C-

C-UM206-MNP (with or without magnetic field treatment) or in response to Wnt-CM as shown by qPCR (supplementary fig 1b).

Cell labelling with L- / C-C-UM206-MNP was then confirmed using immunofluorescence. A clear association between cells and MNP was observed after labelling with either MNP type (Fig. 2a). The viability and metabolism of hMSC bound with L- / C-C-UM206-MNP and exposed to oscillating magnetic fields was then assessed to determine any cytotoxic effects of MNP at a dose shown to induce signalling responses in hMSC. Live/Dead staining was used to determine intracellular esterase activity and cell membrane integrity 14 days after treatment. Cells remain viable after treatment with MNP (L-UM206-MNP or C-C-UM206-MNP) with or without intermittent magnetic field stimulation (Fig. 2b). Magnetic field treatment alone also had no observable effect on cell viability. MTT assay was also used to assess changes in cell metabolism after 14 days treatment (Fig 2c). No overall effects were observed when cells were treated with MNP (L-UM206-MNP or C-C-UM206-MNP) with or without magnetic field stimulation or with magnetic field alone. A dose response study was also performed (supplementary fig. 2). Cells were treated with varying doses of unbound Linear or Cyclic peptide (1-100μg/mL) or with varying doses of L-/C-C-UM206-MNP or uncoated (blank) MNP (5μg to 300μg/2x105 cells). No overall effect on cell metabolism was observed when cells were treated with either MNP or peptide in these dose ranges.

Next, the effects of L- / C-C UM206-MNP on Wnt signalling were assessed. Immunocytochemistry was used to assess nuclear translocation of β-catenin. β-catenin mobilisation was enhanced in cells stimulated with Wnt3a-CM and L-UM206-MNP (and to a lesser extent with C-C-UM206-MNP), demonstrating that L-UM206-MNP are capable of stimulating β-catenin-mediated Wnt signal transduction (Fig 3A). This effect was enhanced when cells were treated with L-UM206-MNP and magnetic field oscillation (Fig. 3B). Next, the effects of L- / C-C-UM206-MNP on the activity of a Wnt TCF/LEF luciferase reporter

which was transiently transfected into hMSC was determined. Six hours after magnetic field stimulation (or treatment with Wnt3a-CM), reporter activity was increased in all groups except for magnetic field only control and cells cultured with Wnt3a-CM and DKK1, a negative regulator of Wnt pathway activation (Fig. 3C(i)). DKK1 effectively inhibited Wnt3A signal transduction, but had no effect on L-UM206-MNP mediated activation. Furthermore, reporter activity was significantly higher when cells were treated with L-UM206-MNP compared to Wnt3a-CM. At 24h, reporter activity in the control groups remained at low levels, whilst Wnt3a-CM significantly increased reporter activity. Reporter activity of L-UM206-MNP stimulated cells persisted 24h after application of the magnetic stimulus and again was not affected by DKK1. In contrast to L-UM206-MNP, C-C-UM206-MNP had a negligible effect on Wnt-reporter activity compared to controls over both time-points (Fig. 3C(ii)).

The mechanism of Wnt pathway activation by UM206-MNP was probed further using a proximity ligation assay to determine the degree of Frizzled receptor clustering in response to MNP. A basal level of receptor clustering was observed in non-treated cells. Treatment with Wnt3a-CM or magnetic field alone had no observable effect on receptor clustering (Fig 4a). In contrast, a noticeable increase in localised receptor clusters was observed in distinct cell populations when cells were treated with L-UM206-MNP, indicating that part of the receptor signal activation may be due to receptor clustering. A reduced level of receptor clustering was observed in response to C-C-UM206-MNP. In contrast control-MNP coated with non-specific IgG had no effect on receptor clustering (supplementary fig. 3a). Co-localisation analysis of MNP and Frizzled2 staining confirmed positive pixel overlap between MNP and Frizzled2 receptors in both L-UM206-MNP and C-C-UM206-MNP treated groups with or without magnetic field (Fig 4b). The extent of MNP/receptor co-localisation was quantified using Manders threshold coefficient which confirmed positive pixel overlap with values

ranging from 0.31 (C-C-UM206-MNP) to 0.48 (L-UM206-MNP). In contrast negligible overlap was observed in IgG-MNP control groups (Manders threshold coefficient =0.025) (supplementary fig. 3b).

The osteogenic response to remote activation of Frizzled2 using L-UM206-MNP was then assessed. MSC labelled with L-UM206-MNP were cultured for 28 days in osteogenic media with intermittent magnetic stimulation. We observed that L-UM206-MNP treated cells formed localised areas of Collagen (Fig. 5A), calcified matrix (Fig. 5B) and Osteocalcin deposition (Fig. 5C) which were less apparent in the non-treated control group. An additive effect on localised matrix formation was observed when cells were treated with L-UM206-MNP with magnetic stimulation. Under our conditions treatment with Wnt3a-CM caused increases in collagen synthesis and Osteocalcin production.

A translational *ex vivo* foetal chick femur model was then used to investigate the potential synergistic effects between a known osteoinductive cue- BMP2 and mechano-activation of the Frizzled receptor. Injection of hMSC alone, or in conjunction with BMP2 releasing microparticles and/or L-UM206-MNP into the femur resulted in formation of secondary mineralisation sites most noticeable in the epiphysis (Fig. 6 A-C). Femurs were subjected to μCT analysis to assess changes in bone volume and density (Fig. 6A). Injection of hMSC alone led to increases in relative bone collar volume but had no overall effect on bone collar density compared to Sham injected control. In contrast, injection of hMSC with BMP2-releasing microparticles, which provided an initial burst release of 60ng BMP2 followed by 10ng/day, resulted in an increase in diaphyseal bone collar density but had no overall effect on bone collar volume (Fig 6b). Wnt pathway stimulation via L-UM206-MNP also resulted in an increase in relative bone collar density but had no overall effect on bone collar volume. The largest effects on bone formation were observed when femurs were injected with L-UM206-MNP labelled MSC along with BMP2 releasing microparticles, which together

caused an overall significant increase in relative bone collar density. Histological analysis of femurs confirmed the presence of secondary calcified mineralisation sites which were prevalent in the cell injected groups (with or without BMP2 and L-UM206-MNP) as shown by Alizarin red staining (Fig. 6C), whilst negligible mineralisation was observed in the sham injected groups. Cell injected groups were also positive for Osteocalcin as shown by Immunohistochemistry (Fig. 6C) and evidence of tissue remodelling by increased collagen and/or sGAG deposition was observed in all cell and L-UM206-MNP / BMP2 injected groups as shown by Alcian blue and Sirius red staining (Fig. 6C).

Discussion

In this study remote targeting and mechano-stimulation of Frizzled receptors for Wnt pathway activation using peptide-conjugated MNP has been demonstrated. It was also shown that this approach offers benefits in a bone tissue engineering context where the promotion of bone formation was achieved. In this investigation, UM206 peptides were coated onto magnetic nanoparticles and used to target MNP to Frizzled receptors at the cell membrane. This allowed remote stimulation of Wnt signal transduction by applying an external magnetic field to oscillate the particle-receptor complex using forces in the piconewton (pN: 10−12N) range as previously calculated [27]. The efficiency of the MNP coating procedure was characterised by examining changes in the physical characteristics of coated MNP and by monitoring unbound protein content in the coating solution supernatants. MNP functionalisation with UM206 peptides resulted in a decrease in free protein and an increase in relative particle size and surface charge. This could be attributed to the peptide layer conjugated to the MNP surface and is consistent with previous work which also showed alterations in MNP properties after functionalisation [14], [28]. Next we examined Frizzled2expression levels in MSC. MSC have previously been shown to express a number of

Wnt ligands and receptors including Frizzled2 [2]. In this study, we also confirmed that MSC stably express Frizzled2 in basal or osteogenic media over three weeks. Our results also suggest that Frizzled2 expression is not regulated by short term stimulation with UM206-MNP or exogenous Wnt3a. This is also consistent with previous work which demonstrated that Frizzled2 expression is not regulated by Wnt3a in hMSC [29]. The potential cytotoxic effects of MNP are an important consideration when developing MNP based tissue engineering treatments. Our experiments show that UM206 peptide alone or MNP bound UM206 with or without magnetic field stimulation has no obvious cytotoxic effects on hMSC at a range of doses. This finding agrees with previous studies which have shown the biocompatibility of iron-oxide based MNP in numerous cell types [30], [31], [32], [33], [34].

Downstream indicators of Wnt pathway activation by UM206-MNP were investigated by assessing β-catenin localisation and end-point activation of TCF/LEF responsive signalling. Our results demonstrate that L-UM206-MNP (and to a lesser extent C-C-UM206-MNP) were capable of initiating nuclear translocation of β-catenin to a similar level as Wnt3a, this is comparable to other studies where Wnt has been shown to initiate β-catenin translocalisation [35]. In addition, our results demonstrate that L-UM206-MNP elevate downstream TCF/LEF expression after 6h which can be maintained up to 24h after treatment. In contrast, Wnt3a marginally elevated pathway activity after 6h but peak activity was observed after 24h, which suggests that L-UM206-MNP mediated activation may initiate a more rapid downstream activation. Interestingly, in contrast with L-UM206-MNP, particles coated with C-C-UM206 peptide had a negligible effect on Wnt reporter activity and only marginally increased β-catenin mobilisation. This may be a result of the lower binding affinity of the cyclic peptide compared to the linear peptide [13]. It is also possible that conjugation of multiple cyclic UM206 ligands to MNP may be inducing steric hindrance which may disrupt receptor binding affinity and reduce the signalling activity of the cyclic peptide.

Our results demonstrated that pathway activation by L-UM206-MNP is not affected by DKK1, an inhibitor of the LRP co-receptor involved in canonical pathway activation, whereas Wnt3a mediated activation was successfully blocked with DKK1. This indicates that LRP is not involved in L-UM206-MNP mediated activation and suggests that MNP stimulate Wnt signalling by an alternative mechanism. This observation is in agreement with our previous work which has shown that antibody-MNP mediated Wnt pathway activation is also independent of LRP receptors [14]. We also employed a PLA assay to assess Frizzled receptor clustering as a potential mechanism by which L-UM206-MNP are inducing Wnt pathway activation. Our results indicate that L-UM206 (and to some extent C-C-UM206) functionalised MNP induce Frizzled2 dimerisation and clustering in distinct cell populations. Previous work from Liu *et al* demonstrated that adherent MSC cultures contain distinct sub-populations which exhibit high endogenous Wnt signalling activity [36]. It is therefore possible that MNP may be inducing receptor clustering in this Wnt receptive population. Further work is required to elucidate the phenotype of these cells. Receptor clustering is a common mechanism of cell signalling activation and has previously been demonstrated using alternate magnetic particle activation systems [37]. Wnt pathway activation by receptor clustering has also been demonstrated in Xenopus embryos where Frizzled3 was found to form active dimers [38]. In contrast to UM206-MNP, no changes in receptor clustering were observed in Wnt3a treated cells. This can be expected as conventional signal activation by Wnt occurs through a complex of Wnt, Frizzled and LRP co-receptors and not necessarily through Frizzled dimers [39]. The mechano-responsiveness and activation of the Wnt pathway has been explored using other approaches. Fluid shear stress or mechanical strain using 4-point bending systems have been shown to initiate β-catenin translocation and activate TCF reporter systems [40], [41]. It is therefore possible that mechano-stimulation of

Frizzled receptors using MNP is enough to induce a signalling response. Taken together, our results suggest a contrasting activation mechanism between MNP and native Wnt ligands.

Our results confirm that Wnt pathway activation plays a role in hMSC osteogenesis. Wnt has been shown to have both inhibitory and promoting effects on MSC osteogenesis [5]. Our recent work utilising immobilised Wnt3a/collagen gel platforms has demonstrated the directional and inductive cues of a Wnt bound platform where MSCs located proximal to the Wnt signal maintain stem cell marker expression whilst migrated cells located distally to the Wnt signal display an osteogenic phenotype [9]. These results also agree with previous work, for example Wnt3a or GSK-3β inhibitors have been shown to promote MSC proliferation and maintain multipotency or promote MSC osteogenesis under certain doses and cellular contexts [6], [7], [42], [43]. In our studies intermittent stimulation of hMSC with L-UM206-MNP over 28 days resulted in localised collagen synthesis, matrix maturation and mineralisation indicating a differentiated osteoblast phenotype. In contrast, treatment with Wnt3a for 28 days resulted in decreased mineralised matrix formation. This discrepancy could be explained by the contrasting dose-response effects of Wnt activation through MNP vs native Wnt. Our data suggest that Wnt pathway activation through L-UM206-MNP is a transient stimulus which is initially beneficial for hMSC lineage commitment to osteogenesis but enables terminal osteoblast differentiation after signal dissipation. Interestingly, this observation mirrors the effects of immobilised Wnt3a on MSC proliferation/differentiation seen by Lowndes *et al* [9] and also agrees with the findings of Ling *et al* [42] and Janeczek *et al* [44] who also showed that a transient Wnt signal is beneficial for hMSC commitment to the osteogenic lineage but withdrawal of Wnt is required for terminal osteoblast differentiation.

The interactions between Wnt and other signalling pathways are complex [45]. Here we investigated the effects of combining Wnt stimulation *via* L-UM206-MNP with BMP2

release from polymer microspheres which have applications in bone tissue engineering [46]. In these experiments we used the foetal chick femur, an established model of endochondral bone development [47], [48]. In this model, bone formation at the bone collar was increased by hMSC injection alone, whilst injection of BMP2 with hMSC or L-UM206-MNP labelled hMSC resulted in increases in bone density, indicating a more mature, functional matrix. The biggest increases in bone density were seen when L-UM206-MNP labelled MSC were co-administered with BMP2 microspheres. During bone formation, Wnt and BMP2 have been shown to act reciprocally to regulate osteoblast differentiation [49]. Our previous work has also demonstrated the anabolic effects of BMP2 releasing microspheres [22]. The link between BMP2 and Wnt signalling has also been demonstrated by Vaes *et al* [50] who found that BMP2 signalling resulted in the upregulation of Wnt antagonists in the late phase of MSC differentiation. Considerable evidence also exists for the activation of TCF/LEF by both BMP/TGF and Wnt during development [51]. Therefore, the ability of L-UM206-MNP plus BMP2 to trigger bone formation could be attributed to the reciprocal relationship between Wnt and BMP signalling, where L-UM206-MNP act to initially trigger lineage commitment whilst BMP2 promotes terminal differentiation. This may explain why a combination of L-UM206-MNP and BMP2 resulted in the greatest enhancement of bone formation. Further work is required to fully explore the downstream signalling events in response to MNP stimulation and to establish the effects of cross-talk between MNP mediated Wnt signalling and the BMP pathway on cell signalling and phenotype.

Using conjugated MNP to activate Wnt signalling may have useful applications as a research tool, in drug discovery and is amenable to translation to the clinic. Due to the expense and difficulty in preparing recombinant Wnt protein, easily synthesised ligands conjugated to magnetic nanoparticles present a viable method for the control of cell signalling and direction of cell differentiation. By initialising Wnt-Frizzled signalling in this manner, UM206-MNP

may be able to over-ride many of the top-level inhibitors of Wnt signalling. Signalling activity can also be enhanced or reduced by operating an external magnetic switch, affording a degree of external control and temporal regulation of pathway activation. This magnetic activation approach has a beneficial impact on bone formation and works in synergy with bone promoting growth factors. This combinatorial strategy which utilises Stem cells with controlled release of clinically relevant growth factors and remote control over cell signalling is particularly attractive due to the relative ease by which this could be administered in the clinic in the form of an injectable cell therapy. Although this approach has particular relevance in bone tissue engineering for fracture repair, the wider applications of minimally invasive injectable cell therapies for tissue engineering are apparent.

Acknowledgements

The authors gratefully acknowledge our collaborators in groups led by Prof. R. Oreffo (University of Southampton), Prof. K. Shakesheff (Nottingham University), Prof. M. Stevens (Imperial College London) and Prof. A. Faussner (Ludwig-Maximilians-University Munich) who kindly donated the TCF/LEF reporter plasmid.

References

1. Oreffo, R.O., et al., *Mesenchymal stem cells: lineage, plasticity, and skeletal therapeutic potential.* Stem Cell Rev, 2005. **1**(2): p. 169-78.
2. Etheridge, S.L., et al., *Expression profiling and functional analysis of wnt signaling mechanisms in mesenchymal stem cells.* Stem Cells, 2004. **22**(5): p. 849-60.
3. Milat, F. and K.W. Ng, *Is Wnt signalling the final common pathway leading to bone formation?* Molecular and Cellular Endocrinology, 2009. **310**(1–2): p. 52-62.
4. Rao, T.P. and M. Kuhl, *An updated overview on Wnt signaling pathways: a prelude for more.* Circ Res, 2010. **106**(12): p. 1798-806.
5. Quarto, N., B. Behr, and M.T. Longaker, *Opposite spectrum of activity of canonical Wnt signaling in the osteogenic context of undifferentiated and differentiated mesenchymal cells: implications for tissue engineering.* Tissue Eng Part A, 2010. **16**(10): p. 3185-97.
6. De Boer, J., H.J. Wang, and C. Van Blitterswijk, *Effects of Wnt signaling on proliferation and differentiation of human mesenchymal stem cells.* Tissue Eng, 2004. **10**(3-4): p. 393-401.

7. Boland, G.M., et al., *Wnt 3a promotes proliferation and suppresses osteogenic differentiation of adult human mesenchymal stem cells.* J Cell Biochem, 2004. **93**(6): p. 1210-30.
8. Qiu, W., et al., *Patients with high bone mass phenotype exhibit enhanced osteoblast differentiation and inhibition of adipogenesis of human mesenchymal stem cells.* J Bone Miner Res, 2007. **22**(11): p. 1720-31.
9. Lowndes, M., et al., *Immobilized WNT Proteins Act as a Stem Cell Niche for Tissue Engineering.* Stem Cell Reports. **7**(1): p. 126-137.
10. Minear, S., et al., *Wnt proteins promote bone regeneration.* Sci Transl Med, 2010. **2**(29): p. 29ra30.
11. Gothard, D., et al., *Tissue engineered bone using select growth factors: A comprehensive review of animal studies and clinical translation studies in man.* Eur Cell Mater, 2014. **28**: p. 166-207; discussion 207-8.
12. Coudreuse, D. and H.C. Korswagen, *The making of Wnt: new insights into Wnt maturation, sorting and secretion.* Development, 2007. **134**(1): p. 3-12.
13. Blankesteijn Wessel Matthijs, L.H., Hackeng Tilman Mathias, *Antagonistic Peptides for Frizzled-1 and Frizzled-2*. 2010: European Patent Office.
14. Rotherham, M. and A.J. El Haj, *Remote Activation of the Wnt/beta-Catenin Signalling Pathway Using Functionalised Magnetic Particles.* PLoS One, 2015. **10**(3): p. e0121761.
15. Akbarzadeh, A., M. Samiei, and S. Davaran, *Magnetic nanoparticles: preparation, physical properties, and applications in biomedicine.* Nanoscale Research Letters, 2012. **7**(1): p. 144-144.
16. Ito, A., et al., *Tissue engineering using magnetite nanoparticles and magnetic force: heterotypic layers of cocultured hepatocytes and endothelial cells.* Tissue Eng, 2004. **10**(5-6): p. 833-40.
17. Lee, E.A., et al., *Application of magnetic nanoparticle for controlled tissue assembly and tissue engineering.* Arch Pharm Res, 2014. **37**(1): p. 120-8.
18. Karahaliloğlu, Z., et al., *Magnetic silk fibroin e-gel scaffolds for bone tissue engineering applications.* Journal of Bioactive and Compatible Polymers. **0**(0): p. 0883911517693635.
19. Wang, Y.-X.J., *Superparamagnetic iron oxide based MRI contrast agents: Current status of clinical application.* Quantitative Imaging in Medicine and Surgery, 2011. **1**(1): p. 35-40.
20. Wimpenny, I., H. Markides, and A.J. El Haj, *Orthopaedic applications of nanoparticle-based stem cell therapies.* Stem Cell Research & Therapy, 2012. **3**(2): p. 1-12.
21. Hughes, S., et al., *Selective activation of mechanosensitive ion channels using magnetic particles.* J R Soc Interface, 2008. **5**(25): p. 855-63.
22. Henstock, J.R., et al., *Remotely Activated Mechanotransduction via Magnetic Nanoparticles Promotes Mineralization Synergistically With Bone Morphogenetic Protein 2: Applications for Injectable Cell Therapy.* Stem Cells Translational Medicine, 2014. **3**(11): p. 1363-1374.
23. Hu, B., A.J. El Haj, and J. Dobson, *Receptor-targeted, magneto-mechanical stimulation of osteogenic differentiation of human bone marrow-derived mesenchymal stem cells.* Int J Mol Sci, 2013. **14**(9): p. 19276-93.
24. Cartmell, S.H., et al., *Development of magnetic particle techniques for long-term culture of bone cells with intermittent mechanical activation.* IEEE Trans Nanobioscience, 2002. **1**(2): p. 92-7.
25. Smith, E.L., et al., *Evaluation of skeletal tissue repair, part 1: assessment of novel growth-factor-releasing hydrogels in an ex vivo chick femur defect model.* Acta Biomater, 2014. **10**(10): p. 4186-96.
26. Smith, E.L., et al., *Evaluation of skeletal tissue repair, part 2: enhancement of skeletal tissue repair through dual-growth-factor-releasing hydrogels within an ex vivo chick femur defect model.* Acta Biomater, 2014. **10**(10): p. 4197-205.

27. Dobson, J., et al., *Principles and design of a novel magnetic force mechanical conditioning bioreactor for tissue engineering, stem cell conditioning, and dynamic in vitro screening.* IEEE Trans Nanobioscience, 2006. **5**(3): p. 173-7.
28. Hu, B., J. Dobson, and A.J. El Haj, *Control of smooth muscle alpha-actin (SMA) up-regulation in HBMSCs using remote magnetic particle mechano-activation.* Nanomedicine, 2014. **10**(1): p. 45-55.
29. Kolben, T., et al., *Dissecting the impact of Frizzled receptors in Wnt/beta-catenin signaling of human mesenchymal stem cells.* Biol Chem, 2012. **393**(12): p. 1433-47.
30. Kanczler, J.M., et al., *Controlled differentiation of human bone marrow stromal cells using magnetic nanoparticle technology.* Tissue Eng Part A, 2010. **16**(10): p. 3241-50.
31. Jeng, H.A. and J. Swanson, *Toxicity of metal oxide nanoparticles in mammalian cells.* J Environ Sci Health A Tox Hazard Subst Environ Eng, 2006. **41**(12): p. 2699-711.
32. Karlsson, H.L., et al., *Size-dependent toxicity of metal oxide particles--a comparison between nano- and micrometer size.* Toxicol Lett, 2009. **188**(2): p. 112-8.
33. Mahmoudi, M., et al., *A new approach for the in vitro identification of the cytotoxicity of superparamagnetic iron oxide nanoparticles.* Colloids Surf B Biointerfaces, 2010. **75**(1): p. 300-9.
34. Moise, S., et al., *The cellular magnetic response and biocompatibility of biogenic zinc- and cobalt-doped magnetite nanoparticles.* Sci Rep, 2017. **7**: p. 39922.
35. Cong, F., et al., *Requirement for a nuclear function of beta-catenin in Wnt signaling.* Mol Cell Biol, 2003. **23**(23): p. 8462-70.
36. Liu, G., et al., *Canonical Wnts function as potent regulators of osteogenesis by human mesenchymal stem cells.* J Cell Biol, 2009. **185**(1): p. 67-75.
37. Mannix, R.J., et al., *Nanomagnetic actuation of receptor-mediated signal transduction.* Nat Nano, 2008. **3**(1): p. 36-40.
38. Carron, C., et al., *Frizzled receptor dimerization is sufficient to activate the Wnt/beta-catenin pathway.* J Cell Sci, 2003. **116**(Pt 12): p. 2541-50.
39. Cong, F., L. Schweizer, and H. Varmus, *Wnt signals across the plasma membrane to activate the beta-catenin pathway by forming oligomers containing its receptors, Frizzled and LRP.* Development, 2004. **131**(20): p. 5103-15.
40. Norvell, S.M., et al., *Fluid shear stress induces beta-catenin signaling in osteoblasts.* Calcif Tissue Int, 2004. **75**(5): p. 396-404.
41. Armstrong, V.J., et al., *Wnt/beta-catenin signaling is a component of osteoblastic bone cell early responses to load-bearing and requires estrogen receptor alpha.* J Biol Chem, 2007. **282**(28): p. 20715-27.
42. Ling, L., V. Nurcombe, and S.M. Cool, *Wnt signaling controls the fate of mesenchymal stem cells.* Gene, 2009. **433**(1–2): p. 1-7.
43. Cook, D.A., et al., *Wnt-dependent osteogenic commitment of bone marrow stromal cells using a novel GSK3beta inhibitor.* Stem Cell Res, 2014. **12**(2): p. 415-27.
44. Janeczek, A.A., et al., *Transient Canonical Wnt Stimulation Enriches Human Bone Marrow Mononuclear Cell Isolates for Osteoprogenitors.* Stem Cells, 2015.
45. Katoh, M., *Network of WNT and other regulatory signaling cascades in pluripotent stem cells and cancer stem cells.* Curr Pharm Biotechnol, 2011. **12**(2): p. 160-70.
46. Kirby, G.T.S., et al., *PLGA-Based Microparticles for the Sustained Release of BMP-2.* Polymers, 2011. **3**(1): p. 571-586.
47. Smith, E.L., J.M. Kanczler, and R.O. Oreffo, *A new take on an old story: chick limb organ culture for skeletal niche development and regenerative medicine evaluation.* Eur Cell Mater, 2013. **26**: p. 91-106; discussion 106.
48. Kanczler, J.M., et al., *A novel approach for studying the temporal modulation of embryonic skeletal development using organotypic bone cultures and microcomputed tomography.* Tissue Eng Part C Methods, 2012. **18**(10): p. 747-60.

49. Bain, G., et al., *Activated beta-catenin induces osteoblast differentiation of C3H10T1/2 cells and participates in BMP2 mediated signal transduction.* Biochem Biophys Res Commun, 2003. **301**(1): p. 84-91.
50. Vaes, B.L., et al., *Microarray analysis reveals expression regulation of Wnt antagonists in differentiating osteoblasts.* Bone, 2005. **36**(5): p. 803-11.
51. Letamendia, A., E. Labbe, and L. Attisano, *Transcriptional regulation by Smads: crosstalk between the TGF-beta and Wnt pathways.* J Bone Joint Surg Am, 2001. **83-A Suppl 1**(Pt 1): p. S31-9.

Fig. 1. **Experimental setup schematic**. **(A)** 250nm SPIO carboxy-dextran functionalised magnetic nanoparticles are covalently coated with UM206 peptide by carbodiimide activation **(B)** Human mesenchymal stem cells (hMSC) are then labelled with UM206-functionalised MNP, labelled cells can then be stimulated with oscillating magnetic fields. Alternatively, MNP-labelled cells can be injected into foetal chick femurs before magnetic field stimulation. **(C)** Alternating time-varied magnetic fields are applied to samples using a bioreactor system consisting of arrays of permanent rare earth magnets which situated beneath the samples.

Fig. 2. **Effects of MNP and magnetic field on cell toxicity and viability**. **(A)** Immunofluorescence images showing L-UM206-MNP (middle) or C-C-UM206-MNP (right) labelled cells, MNP are shown by dextran staining (green). Nuclei are shown by DAPI staining (blue), cell cytoskeleton (red). Images representative of n=3, scale bar represents 50µm. **(B)** Immunofluorescence images showing Calcein-AM (Live) and Ethidium homodimer (Dead) staining after treatment with 25µg of L-/C-C-UM206-MNP, with and without magnetic field after 14 days. Representative images of n=3 shown, scale bar represents 100µm. **(C)** Cell metabolism after treatment with L/C-C-UM206 MNP (with or without magnetic field). Average absorbance values are shown, n=3, error bars represent SEM.

Fig. 3. **L-UM206-MNP activate Wnt signalling**. Immunofluorescence images showing β-catenin mobilisation 24h after stimulation (**A**). Addition of Wnt3A-conditioned media (Wnt-CM) or L-UM206-conjugated MNP resulted in increased nuclear translocation with further increases observed upon magnetic field stimulation. Cell nuclei are shown by DAPI staining (middle row). Scale bar represents 50μm. End point Wnt signalling was assessed using a TCF/LEF luciferase reporter 6h and 24h after treatment **(C)**. Wnt3a-CM increased reporter activity after 6h and 24h (significant), and was blocked by Dickkopf-related protein 1 (DKK1). L-UM206-MNP significantly increased Wnt reporter activity at both time-points and was not affected by DKK1. L-UM206-induced reporter activity was also significantly higher than in Wnt3a-CM groups at 6h **(C(i))**. This dataset is part of a larger dataset part of which has been published previously [14]. Treatment with C-C-UM206 MNP **(C(ii))** had no overall effect on TCF/LEF reporter activity. Error bars represent SEM, n=4. * denotes $p<0.05$, # denotes $p>0.05$.

Fig. 4. **L-UM206-MNP induce Frizzled2 clustering.** Frizzled2 receptor clustering was visualised using a PLA assay 3h after stimulation (**A**). Treatment with 25µg of L- / C-C-UM206-MNP (with or without magnetic field) resulted in clear increases in receptor clustering, whilst treatment with Wnt-CM had no effect. MNP are shown by dextran staining (green), Frizzled2 (red) and cell nuclei by DAPI staining (blue). Representative images of n=3 are shown. Scale bar represents 10µm. Co-localisation analysis of ROI's was used to determine the extent of MNP overlap with Frizzled2 clusters (**B**). Clear regions of co-localisation (indicated by white regions) were observed in cells treated with L- / C-C-UM206-MNP (with or without magnetic field). Quantification of pixel overlap using Manders threshold coefficient for the MNP channel (tM2) confirmed a positive overlap between L- / C-C-UM206-MNP and Frizzled2 clusters. Representative images of n=3 are shown. Error represents SEM.

Fig 5: **L-UM206-MNP enhance matrix production.** An increase in localised collagen deposition (Sirius red) (**A**), nodule formation (Alizarin red) (**B**) and Osteocalcin expression (**C**) was observed after treatment with L-UM206-MNP with magnetic field stimulation. Treatment with Wnt-CM caused an increase in collagen deposition (**A**) but a decrease in nodule formation (**B**), a minor increase in Osteocalcin expression (**C**) was also observed after 28 days. Cell nuclei are shown by DAPI staining, Images representative of n=4. Scale bar represents 200μm.

Fig. 6. **L-UM206-MNP increase bone formation in chick femurs**. (**A**) Injection of BMP2 releasing microparticles (and hMSC) led to increased bone volume but not bone density. Injecting L-UM206-MNP labelled MSC with or without BMP2 resulted in increased bone density, n=8, Error bars represent SEM, * represents $p<0.05$. (**B**) Whole mount images showing calcium deposition (Alizarin red) primarily in the bone collar in all groups. Secondary mineralisation sites were observed at the microinjected epiphyseal regions injected with all hMSC groups. Scale bar represents 1mm. **(C)** Histological sections of all hMSC injected groups displayed evidence of the formation of secondary mineralisation (Alizarin red) as well as tissue remodelling (Alcian blue & Sirius red) and Osteocalcin positive matrix formation in the diaphyseal and epiphyseal injection sites of the femurs after 14 days. Representative images of n=8 shown. Scale bar represents 300 µm (Alizarin red and Alcian blue/Sirius red), 400µm (Osteocalcin).

Figure 1.

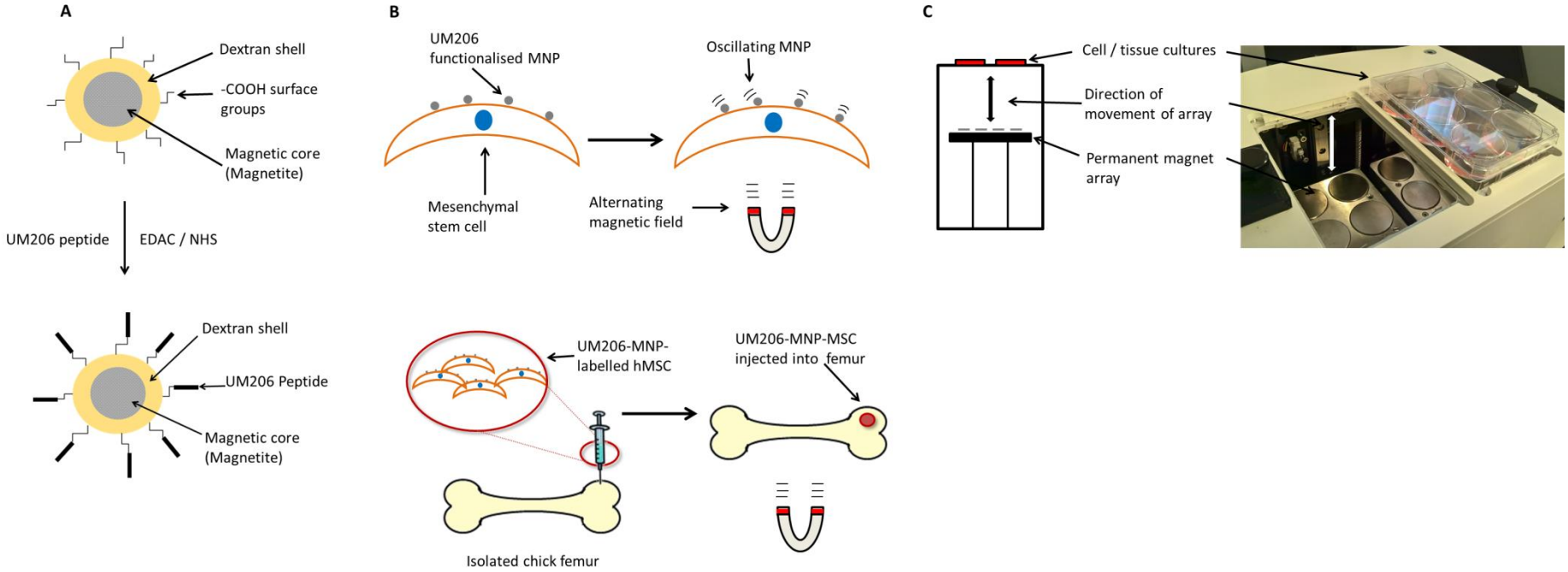
A
Dextran shell
-COOH surface groups
Magnetic core (Magnetite)
UM206 peptide
EDAC / NHS
Dextran shell
UM206 Peptide
Magnetic core (Magnetite)
B
UM206 functionalised MNP
Oscillating MNP
Mesenchymal stem cell
Alternating magnetic field
UM206-MNP-labelled hMSC
UM206-MNP-MSC injected into femur
Isolated chick femur
C
Cell / tissue cultures
Direction of movement of array
Permanent magnet array

Figure 2.

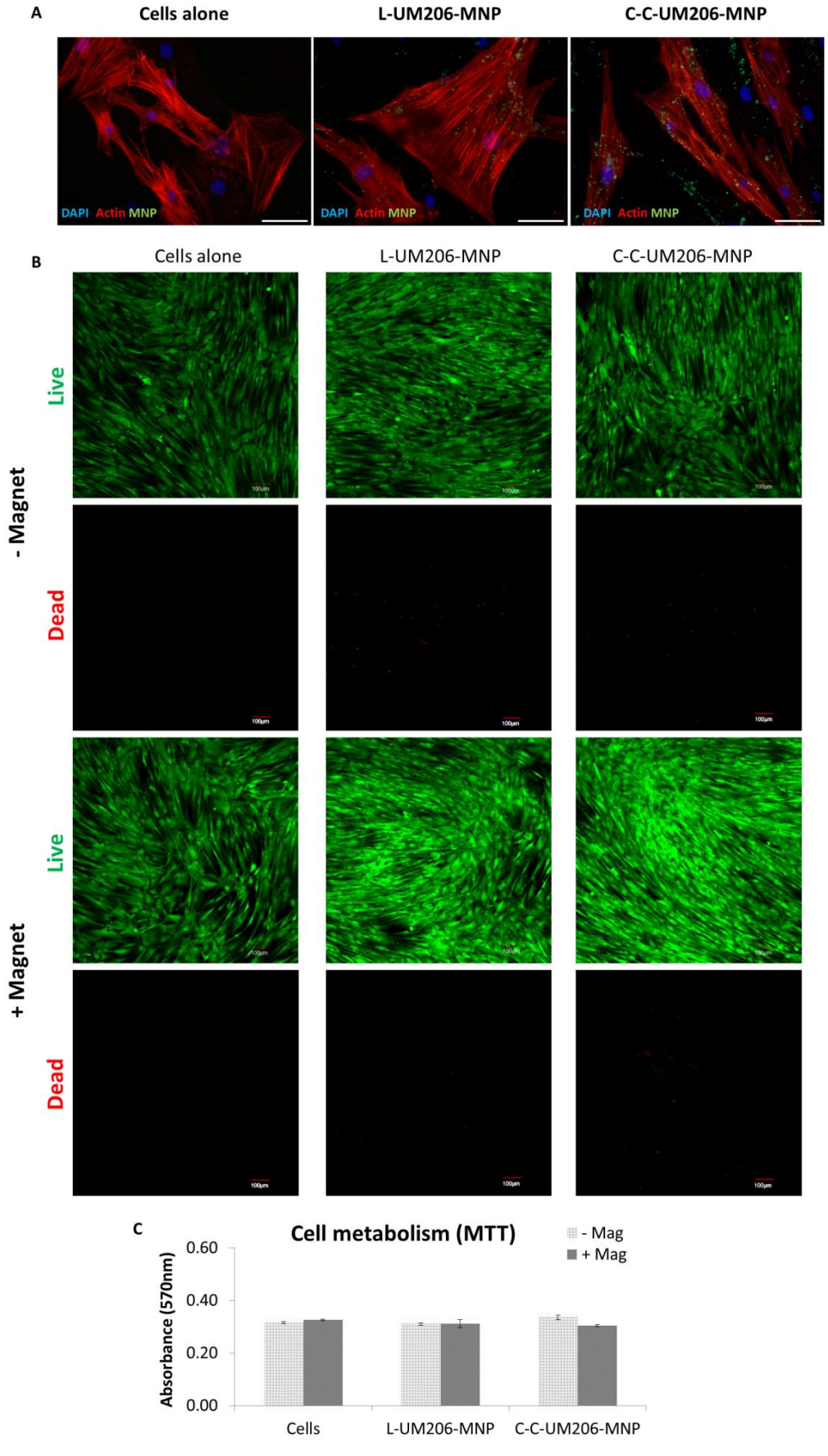
A
Cells alone
L-UM206-MNP
C-C-UM206-MNP
DAPI Actin MNP
DAPI Actin MNP
DAPI Actin MNP
B
Cells alone
L-UM206-MNP
C-C-UM206-MNP
- Magnet
Live
Dead
+ Magnet
Live
Dead
C
Cell metabolism (MTT)
- Mag
+ Mag
Absorbance (570nm)
0.60
0.40
0.20
0.00
Cells
L-UM206-MNP
C-C-UM206-MNP

Figure 3.

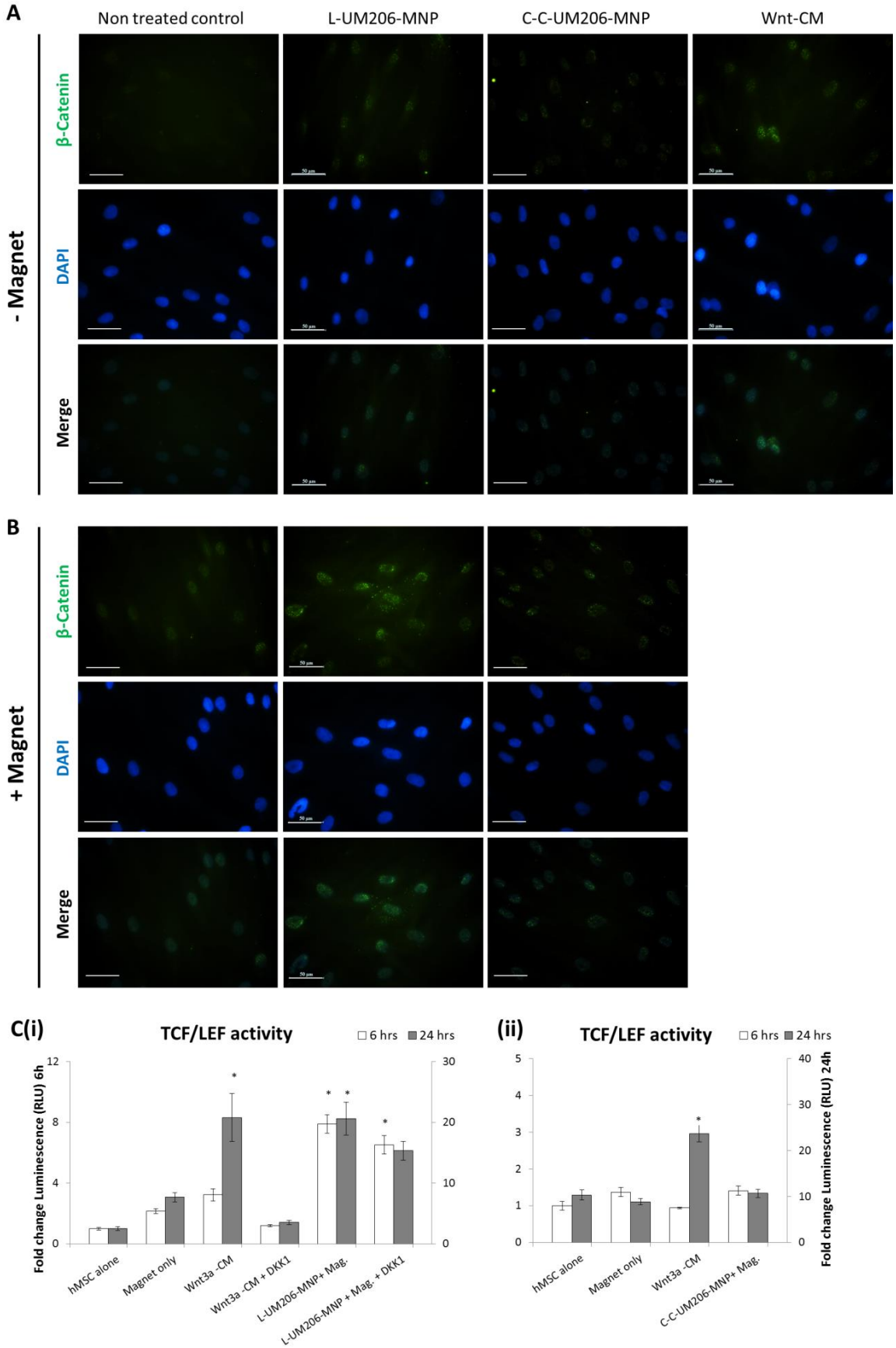
A
Non treated control
L-UM206-MNP
C-C-UM206-MNP
Wnt-CM
- Magnet
β-Catenin
DAPI
Merge
B
+ Magnet
β-Catenin
DAPI
Merge
C(i)
TCF/LEF activity
6 hrs
24 hrs
Fold change Luminescence (RLU) 6h
hMSC alone
Magnet only
Wnt3a -CM
Wnt3a -CM + DKK1
L-UM206-MNP+ Mag.
L-UM206-MNP + Mag. + DKK1
(ii)
TCF/LEF activity
6 hrs
24 hrs
Fold change Luminescence (RLU) 24h
hMSC alone
Magnet only
Wnt3a -CM
C-C-UM206-MNP+ Mag.

Figure 4.

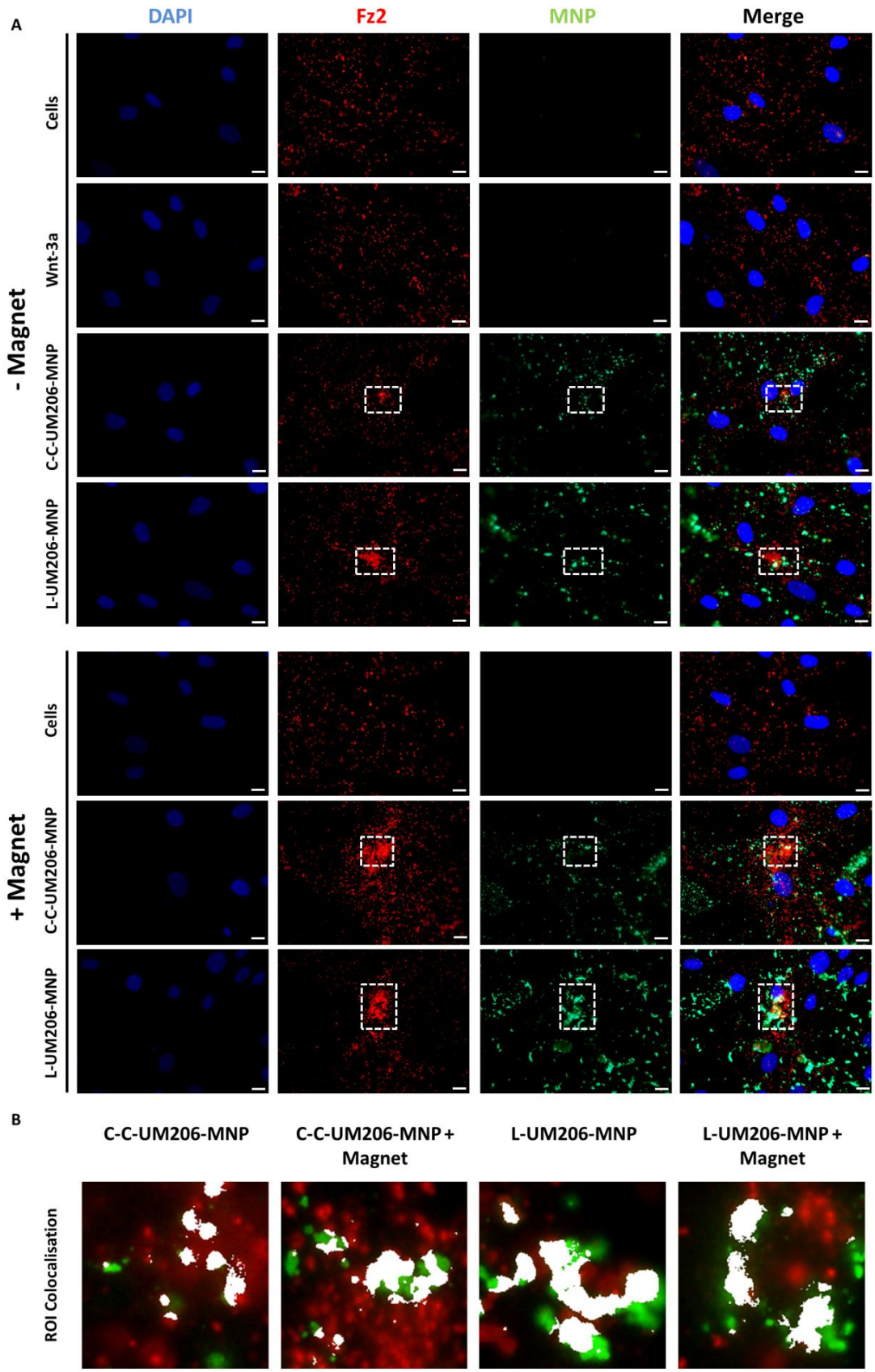

Manders coefficient (tM2)	0.313 ± 0.087	0.445 ± 0.073	0.456 ± 0.070	0.479 ± 0.068

Figure 5.

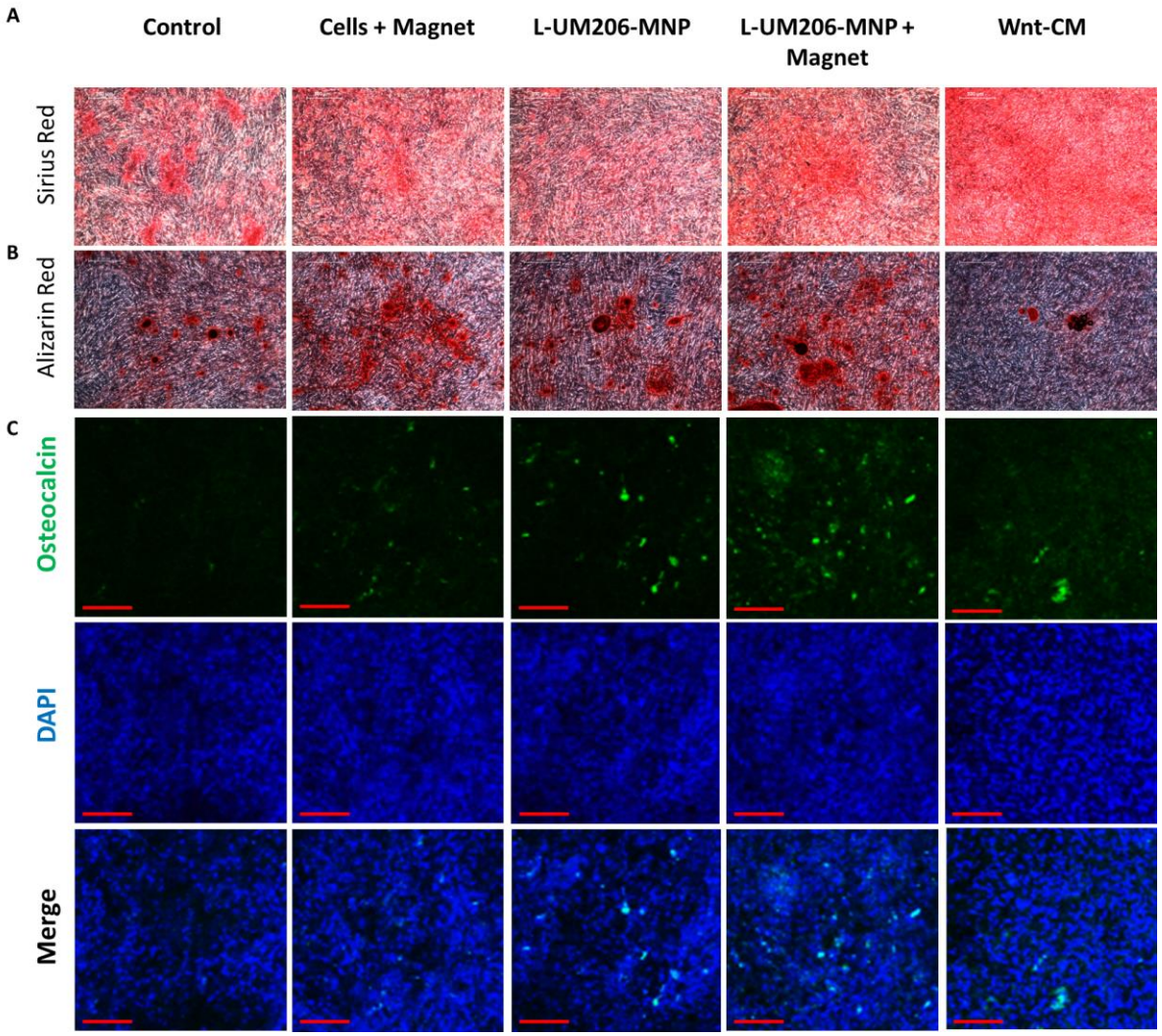
A
Control
Cells + Magnet
L-UM206-MNP
L-UM206-MNP + Magnet
Wnt-CM
Sirius Red
B
Alizarin Red
C
Osteocalcin
DAPI
Merge

Figure 6.

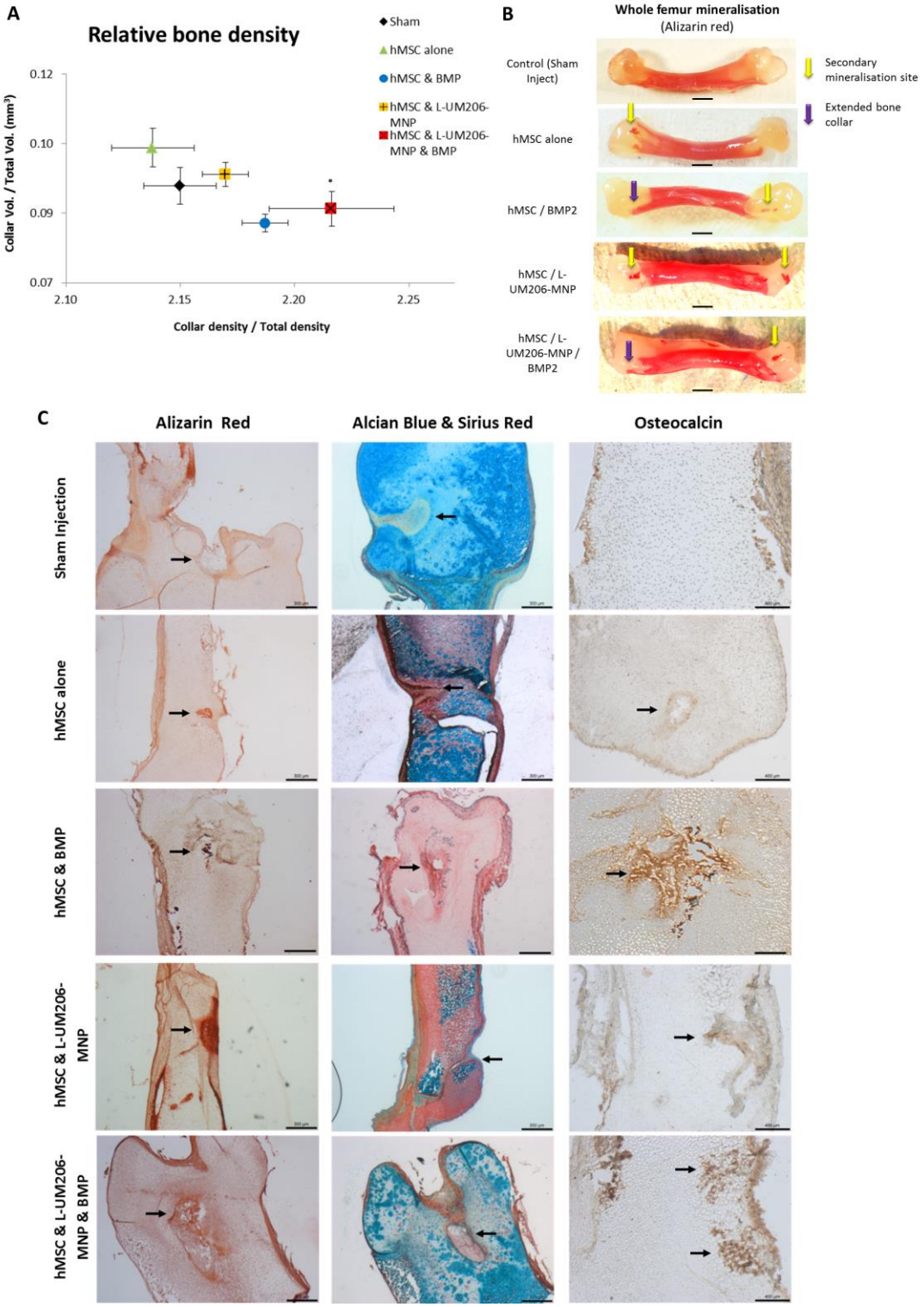
A
Relative bone density
Sham
hMSC alone
hMSC & BMP
hMSC & L-UM206-MNP
hMSC & L-UM206-MNP & BMP
Collar Vol. / Total Vol. (mm³)
0.12
0.10
0.09
0.07
2.10
2.15
2.20
2.25
Collar density / Total density
B
Whole femur mineralisation
(Alizarin red)
Control (Sham Inject)
hMSC alone
hMSC / BMP2
hMSC / L-UM206-MNP
hMSC / L-UM206-MNP / BMP2
Secondary mineralisation site
Extended bone collar
C
Alizarin Red
Alcian Blue & Sirius Red
Osteocalcin
Sham Injection
hMSC alone
hMSC & BMP
hMSC & L-UM206-MNP
hMSC & L-UM206-MNP & BMP